Heliyon 9 (2023) e19474

Contents lists available at ScienceDirect

Heliyon

journal homepage: www.cell.com/heliyon

OPG gene-modified adipose-derived stem cells improve bone formation around implants in osteoporotic rat maxillae

Yingbiao Wan [1], Chen Hu [1], Yongjie Hou, Chenchen Si, Qian Zhao, Zhenzhen Wang, Liyuan Wang, Xiaoqian Guo [*]

General Hospital of Ningxia Medical University, Yinchuan, 750004, Ningxia, China

ARTICLE INFO

Keywords:
OPG
Adipose derived stem cells
Osteoporosis
Dental implantation
Bone repair

ABSTRACT

Background: Osteoporosis is a significant barrier to the use of dental implants in the elderly for the treatment of tooth defects. Adipose derived stem cells (ADSCs) have demonstrated extensive potential for tissue repair and regeneration. The present study aimed to investigate the effectiveness of ADSCs engineered to express high levels of osteoprotegerin (OPG) for the treatment of bone loss in implant dentistry caused by estrogen deficiency.

Methods: A rat model of osteoporosis was established through double oophorectomy, and the rats were treated by gene modified cells Adv-OPG-ADSCs. The effects of the treatment on maxilla tissue changes were evaluated using HE staining and micro-CT. Additionally, ALP and TRAP staining were used to assess osteoblast and osteoclast alterations. Finally, the changes in related osteoblast and osteoclast indicators were measured by RT-qPCR, Western blot, and ELISA.

Results: The successfully generated high-OPG-expressing ADSCs led to increase of cell viability, proliferation, and osteoblast differentiation. Treatment with Adv-OPG-ADSCs significantly ameliorated maxillary morphology, trabecular volume reduction, and bone mineral density decline in the model of estrogen-deficient maxillary implant dentistry. Furthermore, the treatment was beneficial to promoting the generation of osteoblasts and inhibiting the generation of osteoclast. Adv-OPG-ADSCs increased OPG, ALP, OCN, and Runx-2 expressions in the maxilla while suppressing RANKL expression, and also increased the concentration of COL I and PINP, as well as decreased the concentration of CTX-1.

Conclusion: Adv-OPG-ADSCs promote the formation of osteoblasts and inhibit the generation of osteoclasts, thereby inhibiting bone absorption, facilitating bone formation, and promoting the repair of maxillary bone after dental implantation in the presence of osteoporosis-related complications, especially in the setting of estrogen deficiency, providing scientific basis for the application of Adv-OPG-ADSCs in the treatment of implant related osteoporosis.

1. Introduction

Osteoporosis is a systemic and progressive bone disease characterized by normal osteoclast activity, but a significant decrease in the number and activity of osteoblasts, leading to osteopenia and tissue microstructure degeneration, resulting in more fragile bones [1].

* Corresponding author. General Hospital of Ningxia Medical University, No. 804 South Shengli Street, Yinchuan, 750004, Ningxia, China.
E-mail addresses: wanborui@163.com (Y. Wan), guoxiaoqian100@126.com (X. Guo).

[1] Equal contributors and they contributed as co-first authors.

https://doi.org/10.1016/j.heliyon.2023.e19474
Received 25 April 2023; Received in revised form 14 August 2023; Accepted 23 August 2023
Available online 2 September 2023

This condition is mainly due to aging, inflammation, heredity, hormone imbalance and malnutrition [2]. Osteoporosis and low bone mass are more prevalent in women compared to men [3]. Reports indicate that one-third of women worldwide aged 50 or above suffer from osteoporotic fractures [4]. Postmenopausal women may experience estrogen deficiency, which is closely associated with osteoporosis. Estrogen deficiency can result in elevated osteoblast apoptosis, bone loss, and ultimately osteoporosis [5]. Currently, drug therapy for osteoporosis includes the use of estrogen agonists/antagonists, bisphosphonates, receptor activator of nuclear factor kappa-B ligand (RANKL) inhibitors, parathyroid hormone-receptor agonists, and sclerostin inhibitors [6]. Dental implant therapy is a common clinical method for repairing missing teeth, which is very popular among patients. However, the failure rate of treating elderly patients with dentition defects or missing teeth is high, with successful patients mostly limited to young patients [7]. Elderly patients might have bone metabolic diseases such as osteoporosis, which causes bone loss, and decrease bone density, which can result in an unstable and reduce the fixation strength [8]. Therefore, adding agents to assist maxillary bone regeneration while using implants is necessary to strengthen bone repair and reconstruction in elderly patients with bone metabolic diseases [9].

Adipose derived stem cells (ADSCs) are mesenchymal stem cells that are isolated from human or animal adipose tissue [10,11]. Among various mesenchymal stem cells (MSCs), ADSCs have broad application potential in tissue repair and regeneration [12]. They have the ability to self-renew and differentiate into multiple cell lines, including adipocytes, osteoblasts, and chondrocytes, and are therefore considered to have significant therapeutic potential [13]. Additionally, they can secrete a variety of nutritional factors, cytokines, and chemokines, playing an important role in nerve repair, inflammatory regulation, and immune regulation [14,15]. ADSCs improve the microstructure of osteogenic and vascular-deprivation-induced osteonecrosis tissue, thereby enhancing bone regeneration in cases of vascular necrosis of the femoral head in rabbits [16]. Many studies have reported that genetically modified ADSCs can be used to treat bone metabolic diseases [17].

Osteoprotegerin (OPG), which is encoded by the TNFRSF11B gene, is a secreted member of the TNF receptor protein superfamily and is expressed in multiple tissues. However, its role in bone metabolism was initially discovered [18]. OPG plays a crucial role in bone repair by preventing RANKL from binding to receptor activator of nuclear factor kappa-B (RANK) and inhibiting osteoclast activity and maturation, thereby reducing excessive bone resorption and promoting bone formation [19]. Moreover, osteoprotegerin proteins are involved in other physiological and pathological processes, including vascular calcification, immune regulation, and tumor progression [20–22]. Based on the above report, we hypothesized that high-expression of OPG in ADSCs could improve maxillary bone repair in an ovariectomy (OVX)-treated rat. An osteoporosis rat model was established by oophorectomy, and the hypothesis was verified by using OPG-modified ADSCs to repair bone loss around the implant. Therefore, the study's objective is to construct ADSCs that high-express OPG to improve maxillary bone loss and remodeling, enhance oral implantation, and provide a reliable basis for clinical oral implantation treatment of tooth loss in patients with osteoporosis.

2. Materials and methods

2.1. Construction of OVX rat model and study design

We established an animal model of osteoporosis in the mandible by ovariectomy. Then we infected ADSCs with adenovirus highly expressing OPG and injected OPG gene modified ADSCs into the maxillary implant crevice of osteoporotic rats. All animals were treated in accordance with the Guide for the Care and Use of Laboratory Animals, and all animal investigation protocols were approved by the Research Ethics Committee of Ningxia Medical University General Hospital (Approval No.: 2020-131).

The rats were divided into three groups, a normal group of six, which did not undergo any intervention; a sham group of six, which received ovariectomy surgery, but did not have their ovaries removed; and an OVX group of twenty-four, which underwent bilateral oophorectomy in accordance with FDA guidelines. Rats underwent OVX and their teeth (the first molar) were extracted after 8 weeks post-surgery. After a 4-week recovery period, dental implants (2 mm diameter, 4 mm length, 2.6 mm head diameter) were performed. The rats were still divided into three groups, the OVX + PBS group, where injections a certain amount of PBS were administered during dental implantation; the OVX + Adv-ADSCs group, where injections of Adv-ADSCs were administered during dental implantation; and the OVX + Adv-OPG-ADSC group, where injections of Adv-OPG-ADSCs were administered during dental implantation (Fig. S1A).

Specifically, to establish an OVX model in rats, a bilateral oophorectomy was performed. The rats were anesthetized using pentobarbital sodium (45 mL/kg) via intraperitoneal injection. After securing the rats on the operating table, the ovaries were exposed following surgical standards, and both ovaries were removed after ligating the fallopian tube at the lower end of the ovary to create the OVX group. In the sham surgery group, only a small amount of adipose tissue was removed, and the ovaries were left intact. Penicillin 200000 units were administered via intramuscular injection before the surgery.

The remaining 18 OVX-treat rats in the group mentioned above have already undergone OVX, and their first molars were removed 8 weeks after surgery. After a 4-week recovery period, dental implants (diameter 2 mm, length 4 mm, head diameter 2.6 mm) were performed. Using a pilot drill, a hole was prepared in the site of the previous extraction. The implant was inserted into the hole. The rats were still divided into three groups: the OVX + PBS group of 6 rats injected with physiological saline during the tooth implantation period; the OVX + Adv-ADSCs group composed of 6 rats injected with cell suspension containing Adv-ADSCs during the tooth implantation period; and the OVX + Adv-OPG-ADSC group of 6 rats injected with cell suspension containing Adv-OPG-ADSCs during the tooth implantation process. Specifically, after culturing the Adv-OPG-EGFP infected ADSCs for 2 days, the cells were collected after being washed with PBS and the cell concentration was adjusted to 1×10^7 cells/mL. In the OVX + Adv-OPG-ADSCs group, 100 μL of Adv-OPG-EGFP transfected ADSCs were injected into the submucosa around the implant. Similarly, after culturing the Adv-ADSCs for 2 days and washing with PBS, the cells were collected and the cell concentration was adjusted to 1×10^7 cells/mL. In the OVX + Adv-ADSCs group, the hole was prepared in the same way as before, and an equal amount (100 μL) of Adv-ADSCs suspension was injected

into the submucosa around the implant. In the OVX + PBS group, the same method of hole preparation was used, and an equal amount (100 μL) of PBS was injected into the submucosa around the implant. After treatment, the soft diet and sterile water were fed to the rats for 3 weeks, and then they were euthanized with an overdose of pentobarbital and cervical dislocation at the dislocation site. Corresponding maxillary bone tissue was collected, with a portion undergoing micro-CT scans and histological studies, and another portion undergoing molecular experiments such as Western blotting.

2.2. Isolation and culture of allogeneic ADSCs

Primary ADSCs were isolated from the adipose tissue of rats and cultured. The fat tissue surrounding the kidneys and testicles of 4-week-old Sprague-Dawley rats was carefully separated. After removing any visible blood vessels, the tissue was finely chopped and digested using collagenase type II (0.15% w/v) in KRBH buffer for 60 min at 37 °C while shaking. Subsequently, floating adipocytes were separated by centrifugation at 1200 rpm for 5 min. The isolated ADSCs were then cultured in flasks with DMEM medium containing 10% FBS, 100 U/mL penicillin, and 0.1 mg/mL streptomycin at 37 °C in a humidified atmosphere with 5% CO_2. The culture medium was replaced every three days, and primary cells were passaged twice. Then, ASDCs were analyzed by flow cytometry to identify cell characterization.

2.3. Induction of osteogenic differentiation and adipogenic differentiation

Allogeneic ADSCs were cultured in an incubator at 37 °C and 5% CO_2. When the degree of cell fusion reached 80–90%, the cells were digested with 0.25% Trypsin-0.04% EDTA and then inoculated into six-well plates coated with 0.1% gelatin. The cell density was 2×10^4 cells/cm^2, and 2 mL of complete medium was added to each well and placed inside the incubator. When cell alignment reached 60–70% and complete medium was absorbed, 2 mL of rat adipose mesenchymal stem cells were added into the bone differentiation medium (RASMX-90021, Cyagen). In the control group, L-DMEM culture with 10% embryo bovine serum content was used. In the adipogenic differentiation, when the cell confluence reached 80–90%, 2 mL of Lipogenic condition medium (RAXMD-90031, Cyagen) was added, and for the control group, L-DMEM medium containing 10% fetal bovine serum was added.

Two groups were updated every three days on average. The induction period lasted from 2 to 4 weeks. Lipid accumulation was assessed using oil red O staining for 40 min at room temperature. Calcium node formation was evaluated using Alizarin red staining based on cell morphology and growth conditions.

2.4. Genetic modification of allogeneic ADSCs

The rat OPG gene including enzymatic sites (AgeI & NheI) was synthesized by BGI (Beijing, China) and cloned into the GV315 transferring plasmid (Supplementary materials). Then the reconstructed plasmid was co-transfected with the packaging plasmid (pBHGlox ΔE1, 3Cre; Microbix, Canada) into HEK293 cells. Through Cre/loxP system, AdV genes and OPG gene were recombinated in HEK293 cells, following which, viral particles were released into the medium. This medium was harvested, and the viral particles harboring OPG gene were isolated and purified through CsCl gradient centrifugation. The isolated virus AdV-OPG was amplified and titrated (1×10^{10} PFU/mL). Adenoviral infection was carried out when ADSCs reached 50–70% confluence. ADSCs were infected with green fluorescent protein (GFP)-empty (ADSCs-v) or OPG expressing adenoviral vector (ADSCs-OPG) at a multiplicity of infection (MOI) of 10. The infected cells were then incubated overnight under standard conditions and the medium was changed. The expression of the EGFP reporter gene was analyzed at 24, 48, and 72 h after transduction. The transduced group and control group consisted of the OPG-transduced and untransduced ADSCs, respectively. Through observing under a fluorescence microscope and based on EGFP expression, the efficiency of adenovirus infection was evaluated by counting the percentage of EGFP positive cells, which reached >98%. All experiments and cell number determinations were conducted in triplicate.

2.5. Micro computed tomography (CT) analysis

The maxilla is fixed in 4% paraformaldehyde for 48 h. The maxilla was assessed using a conus beam micro-CT system scan, the Hounsfield unit gray threshold was calculated using skyscan analysis software, and bone trabecular volume (BV/TV), bone trabecular number (Tb. N), bone trabecular thickness (Tb.Th), and bone mineral density (BMD) were determined using a three-dimensional region of interest (ROI). Finally, the 3D image of the sample is reconstructed using CTvox software (Bruker, Belgium).

2.6. Hematoxylin-eosin (HE) staining

Formalin-fixed maxillae were decalcified in a 10% EDTA solution for 30 days at 4 °C. Maxillary bone tissues were embedded in paraffin and cut into 4 μm sections, stained with standard hematoxylin and eosin (HE), or stained for alkaline phosphatase activity, or stained for tartrate-resistant acid phosphatase.

Following the conventional HE staining method (Shanghai Qianyakangyao Biotechnology, BH0001), sections were dewaxed in water and then stained with hematoxylin and eosin. After dehydration and sealing, the sections were observed using an optical microscope. Morphological parameters of bone tissue were analyzed using pathological image analysis software.

2.7. ALP staining

We sliced different groups of tissues and determined the activity of ALP through immunohistochemistry. The paraffin section was dewaxed using conventional methods and then immersed in citric acid antigen retrieval buffer (pH 6.0, Shanghai Qianyakangyao Biotechnology, B0034) and microwaved for antigen retrieval. The sections were then treated with hydrogen peroxide (3%) to block endogenous peroxidase. The tissue was circled using a histochemical pen and covered with 3% BSA dropwise for 30 min. The primary antibody, Anti-ALP antibody (Affinity, DF12525), was added and incubated overnight at 4 °C, followed by incubation with the secondary antibody (Abcam, ab205718) at room temperature for 50 min. The DAB chromogenic solution (Agilent, K3468) was then added dropwise, and the positive brownish-yellow color under the microscope indicated the termination of color development. Hematoxylin was used for counterstaining for 30 min. The hematoxylin differentiation solution was differentiated for a few seconds, and the hematoxylin re-blue solution was used for re-blueing. Finally, the section was dehydrated and sealed.

2.8. TRAP staining

Osteoclast levels can be detected using TRAP staining. To prepare the TRAP incubation solution (Shanghai Qianyakangyao Biotechnology, BH0020), the paraffin sections were first dewaxed to water. Then, the solution was made by combining 1 mL of hexaazo byfuchsin, 18 mL of acetic acid buffer, 1 mL of naphthol AS-BI phosphate solution, and 0.282 g of potassium sodium tartrate. The mixture was mixed well and added to the histochemical circle for incubation, and osteoclasts were observed under optical microscopy. Subsequently, the nuclei were stained with hematoxylin staining and the samples were dehydrated and sealed. The examination was performed under a microscope, and images were acquired for analysis. TRAP-positive cells were visualized and TRAP positive cells that have more than 3 nuclei were counted as TRAP-positive multinucleated cells ($TRAP^+$ cells).

2.9. ALP activity

The activity of alkaline phosphatase (ALP) in Adv-ADSCs and Adv-OPG-ADSCs was measured using an ALP activity kit (P0321 M, Beyotime, Shanghai, China). Specifically, cell lysis buffer is used to lyse cells. After co injection of the extract and *p*-nitrophenol at 37 °C for 30 min, its activity was measured at a wavelength of 405 nm. ALP activity was evaluated based on the absorbance value obtained.

2.10. Western blotting

Western blotting was used to analyze the total protein from the Maxillary bone. The tissue surrounding the maxillary second molar was placed in RIPA lysis buffer (Beyotime, Shanghai, China) containing 1% PMSF, and steel balls were added to grind the tissue. After centrifugation to remove insoluble material, the supernatant was collected. BCA protein assay was performed for protein quantification. Samples were denatured in SDS-PAGE sample loading buffer for 5 min, and SDS-PAGE was carried out on a 10% gel that was subsequently transferred to a PVDF membrane. The membrane was blocked with 5% skim milk and then incubated with primary antibody overnight at 4 °C. The primary antibodies used were anti-OPG (Affinity, DF6824, 1:2000), anti-RANKL (Affinity, AF0313, 1:3000), anti-RANK (CST, 4845S, 1:2000), anti-ALP (Affinity, DF12525, 1:2000), anti-OCN (Affinity, DF12303, 1:2000), anti-Runx2 (Affinity, AF5186, 1:2000), and anti-GAPDH (Affinity, AF7021, 1:5000). After incubation with a horseradish peroxidase-conjugated secondary antibody (Beyotime, A0192, 1:3000) for 1 h at room temperature, chemiluminescence detection was employed. Image analysis software was used for quantitative analysis of the protein bands.

2.11. Reverse transcription quantitative polymerase chain reaction (RT-qPCR)

Tissue surrounding the maxillary second molar was collected using a surgical microscope and homogenized using a tissue homogenizer (OMAI). According to the manufacturer's protocol, total RNA was isolated from tissue using Trizol reagent (Invitrigen, 15596026). RNA was reverse transcribed into complementary DNA employing a reverse transcription system. qPCR was performed using ChamQ Universal SYBR qPCR Master Mix (Vazyme, Q711-02). The reaction conditions were as follows: 90 °C for 5 min and 5 s, respectively. 60 °C for 90 s, 40 cycles. The primers used were as listed in Table 1.

Table 1
Sequences of primers used for RT-qPCR.

Primers	Sequence (5′-3′)
OPG-Forward	TGTCCCTTGCCCTGACTACT
OPG-Reverse	CACATTCGCACACTCGGTTG
RANKL-Forward	CCTGTACTTTCGAGCGCAGA
RANKL-Reverse	AGTCGAGTCCTGCAAACCTG
GAPDH-Forward	GAAGGTCGGTGTGAACGGAT
GAPDH-Reverse	ACCAGCTTCCCATTCTCAGC

2.12. Clone formation assay

Cell proliferation of Adv-ADSCs and Adv-OPG-ADSCs was assessed with clone formation assay. Adv-ADSCs and Adv-OPG-ADSCs were seeded at a density of 1000 cells per well in a 6 well plate, and treated after 12 h. After 10 days of culture in the incubator, the cells were washed with PBS, fixed with 75% ethanol for 15 min, and then stained with Crystal violet staining solution for 25–30

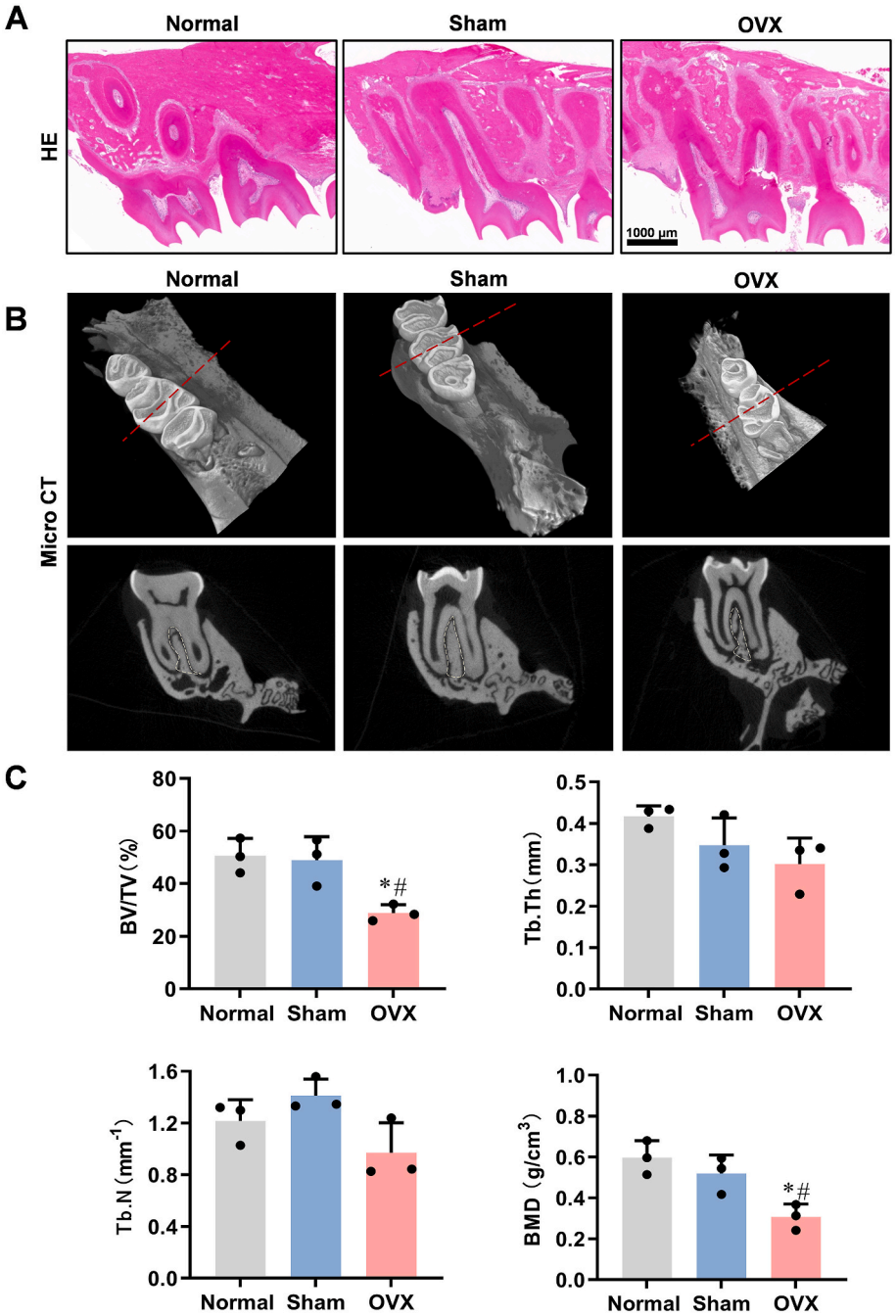

Fig. 1. Morphology and bone quality analysis of the maxillary bone in a rat model of osteoporosis. (A) Hematoxylin eosin (HE) staining of bone tissue around the maxillary teeth. Scale bars represent 1000 μm. (B) Representative images of the longitudinal maxillary morphology of OVX-treated rats were examined by micro-CT. The red dashed line indicates the location of the tomography scan (C) Measurement and analysis of bone trabecular volume (BV/TV), bone trabecular number (Tb. N), bone trabecular thickness (Tb.Th), and bone mineral density (BMD) of the maxillary bone in OVX-treated rats; All data are mean ± standard deviation, n = 3, *P < 0.05, compared to Normal group. #P < 0.05, compared to Sham group.

min. After washing with deionized water for three times, observe and count the cell colonies formed on the Petri dish under the microscope.

2.13. CCK-8

As per the manufacturer's instructions, cell counts were conducted at 0, 12, 24, 48, and 72 h (n = 3) using CCK-8. The prepared culture medium was supplemented with ADSCs (at a density of 1×10^5 cells per well) and then inoculated into each well of a 48 well plate. CCK-8 solution (50 μL) was added to each group and then they were incubated at 37 °C and 5% CO_2. After incubation for 2 h, the ADSCs were rinsed with PBS to eliminate background interference. Then, the microplate reader was used to read the wavelength of ADSCs inoculated on each scaffold at a wavelength of 450 nm.

2.14. Enzyme-linked immunosorbent assay

Homogenized maxilla was used for ELISA experiments. As per the instruction manual of the assay kit (Shanghai Tongwei biotechnology CO., Ltd), quantification of COL I, PINP, and CTX-1 was carried out. The tissue samples were measured either in duplicates or single detection, depending on sample availability.

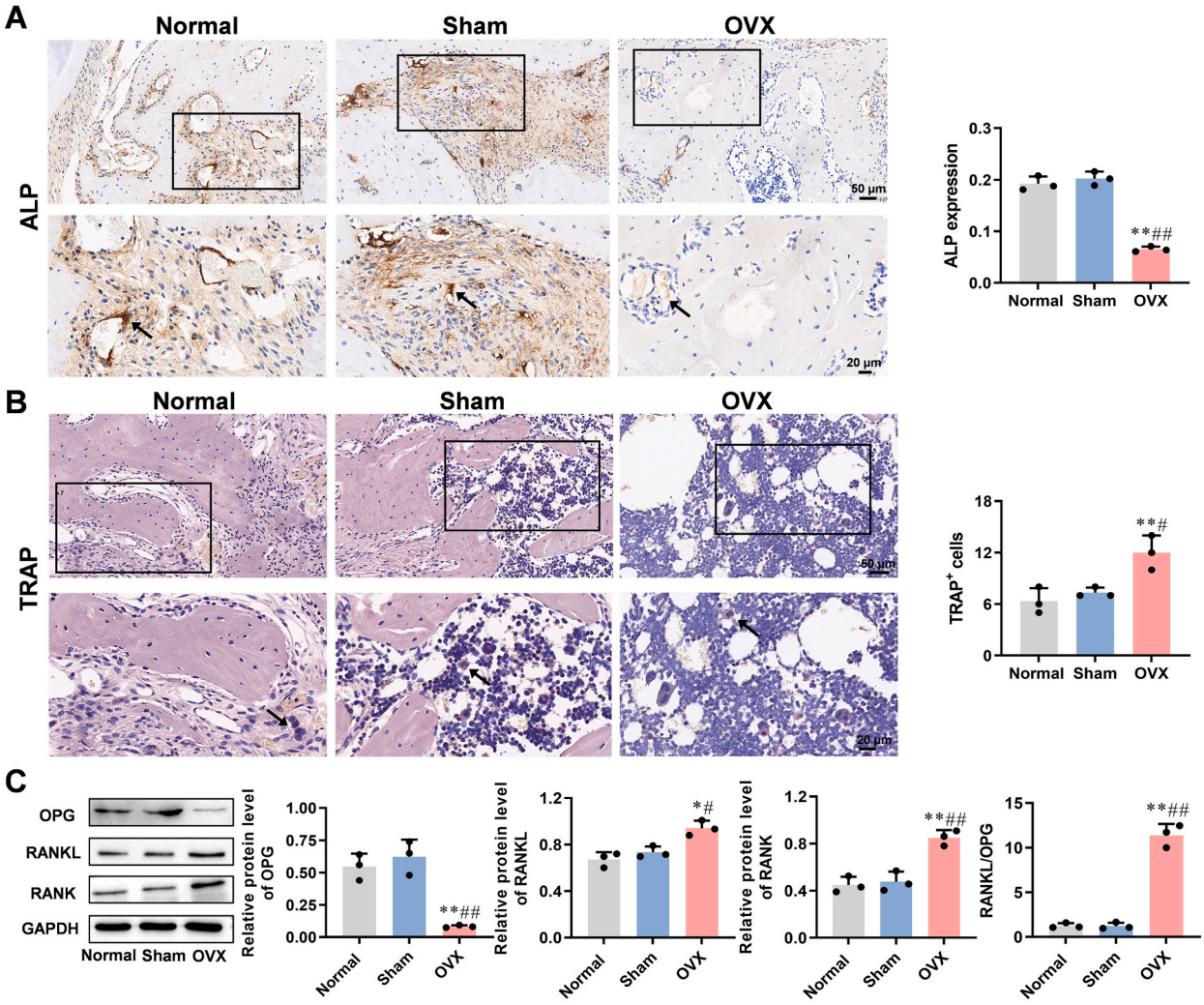

Fig. 2. Analysis of osteoblasts and osteoclasts in the maxillary bone of osteoporosis model rats. (A) Analysis of ALP in the maxillary bone of osteoporosis model rats were examined by immunohistochemistry. Scale bars represent 50 μm (upper panel) and 20 μm (lower panel). (B) TRAP staining analysis was performed on the maxillary bone of osteoporosis model rats to identify osteoclasts. Scale bars represent 50 μm (upper panel) and 20 μm (lower panel). (C) The protein levels of OPG, RANK, RANKL in bone tissue around the maxillary teeth were analyzed by western blotting. *P < 0.05, **P < 0.01, compared to Normal group. All data are mean ± standard deviation, n = 3, #P < 0.05, ##P < 0.01, compared to Sham group.

2.15. Statistical analysis

The data were analyzed using GraphPad Prism8 and presented as mean ± standard deviation (SD). The difference of means between groups was compared using one-way analysis of variance (ANOVA), followed by post hoc Tukey (least significant difference) tests. A *P*-value of less than 0.05 was considered statistically significant.

3. Results

3.1. The animal model for maxillary bone osteoporosis was established, resulting in maxillary bone loss

To evaluate the effects of osteoporosis, we used ovariectomized rats as our osteoporosis models and performed histological verification using HE staining and micro-CT. Compared to the Sham group, the OVX group showed the number of bone trabeculae in maxilla was reduced and the density of bone structure was reduced by HE staining (Fig. 1A). micro-CT results show that, compared with the Sham group, the maxillary bone volume is slightly reduced in the OVX group, and there is a slight decrease in bone between the roots (Fig. 1B). The bone trabecular volume (BV/TV) and bone mineral density (BMD) of bone trabeculae were significantly reduced. Although the difference was not statistically significant, the thickness of trabeculae (Tb. Th) and the number of trabeculae (Tb. N) were also lower (Fig. 1C).

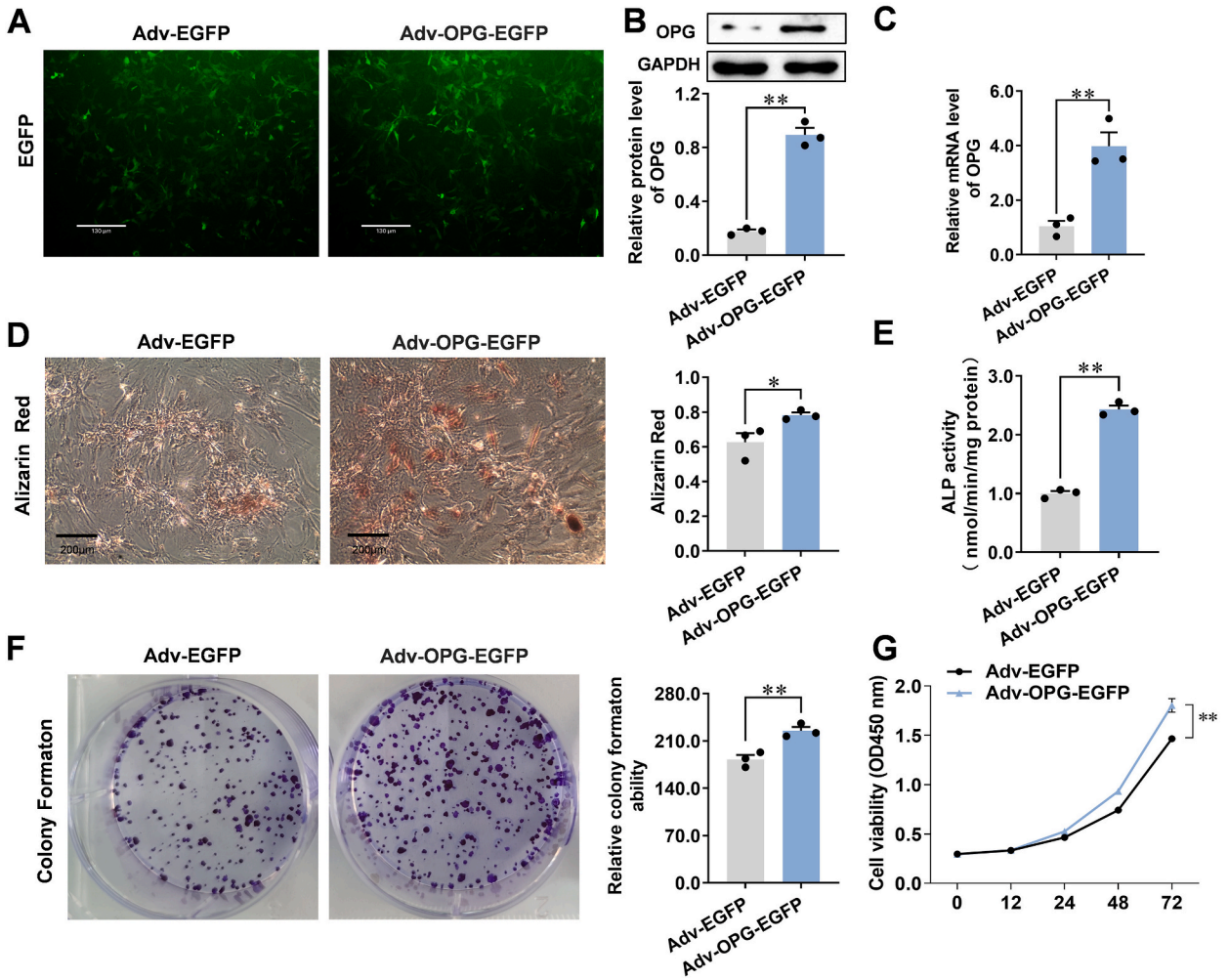

Fig. 3. Identification of OPG modified ADSCs (Adv-OPG-ADSCs). (A) EGFP fluorescence was employed to detect the transfection efficiency in Adv-EGFP group and Adv-OPG-EGFP group. Scale bars represent 130 μm. (B) The level of OPG protein in Adv-OPG-ADSCs was detected by Western blotting. (C) RT-qPCR was used to detect the mRNA level of OPG in Adv-OPG-ADSCs. (D) Alizarin red staining was employed to evaluate the differentiation of osteoblasts in Adv-OPG-ADSCs. Scale bars represent 200 μm. (E) Alkaline Phosphatase Assay Kit was used to detect ALP activity in Adv-OPG-ADSCs. (F) Cell growth of Adv-OPG-ADSCs was measured by colony formation assays. (G) The cell viability of Adv-OPG-ADSCs was detected using CCK-8; All data are mean ± standard deviation, n = 3, *P < 0.05, **P < 0.01, compared to Adv-EGFP group.

3.2. The bone surface of the maxilla in osteoporotic rats shows an increase in osteoclasts, a decrease in osteoblasts

After immunohistochemistry and ALP staining, it was found that the ALP expression of the OVX group was significantly reduced compared to the Sham group, indicating a significant decrease in osteoblasts (Fig. 2A). The TRAP staining results showed an increase in TRAP activity in the OVX group when compared with the Sham group, indicating a significant increase in osteoclasts in the OVX group

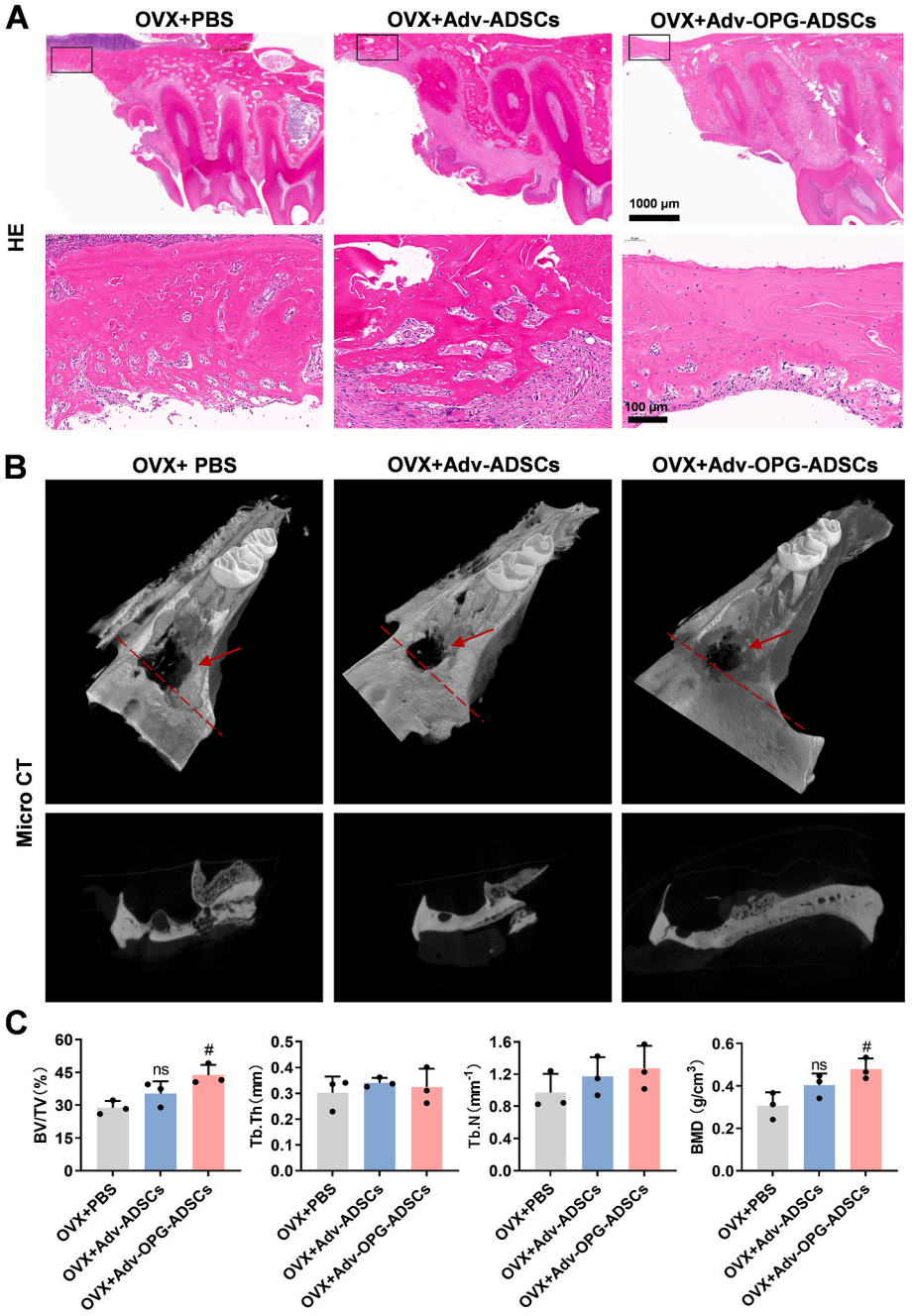

Fig. 4. Adv-OPG-ADSCs promoted bone formation and reduced bone defects in maxilla of osteoporosis rats. (A) HE staining of bone tissue around maxillary teeth. Black rectangles are areas near the extracted dental implants. Scale bars represent 1000 μm (upper panel) and 100 μm (lower panel). (B) Representative 3D images and tomographic images of the longitudinal maxillary morphology of OVX-treated rats were examined by micro-CT. The red dashed line indicates the location of the tomography scan, and the red arrow indicates the location of the dental implant extraction. (C) Measurement and analysis of bone trabecular volume (BV/TV), bone trabecular number (Tb. N), bone trabecular thickness (Tb.Th), and bone mineral density (BMD) of the maxillary bone in OVX-treated rats; All data are mean ± standard deviation, n = 3, $^{\#}P < 0.05$, compared to OVX + PBS group.

(Fig. 2B). Western blotting results indicated that compared to the Sham group, the protein expression level of OPG decreased in the OVX group, whereas RANKL and RANK levels increased (Fig. 2C).

3.3. Construction and identification of OPG-modified ADSCs

To identify ADSCs, we analyzed the specific surface antigens of ADSCs using flow cytometry. The results revealed that ADSCs tested positive for CD29 and CD90 surface antigens, with percentages of 100%. Additionally, no CD45 surface antigen was expressed by ADSCs (Fig. S1B). Consequently, we successfully isolated and cultured ADSCs in vitro. Subsequently, we measured their ability to differentiate into adipogenic and osteogenic cells (Fig. S1C). To determine the characteristics of Adv-OPG-EGFP modified ADSCs, we tested their ability to express OPG and transform into osteoblasts, as well as their cell viability and proliferation ability. The results demonstrated that the infection efficiency in the Adv-EGFP group and the Adv-OPG-ADSCs group are qualified (Fig. 3A). We found that the results of Western blotting and RT-qPCR showed significantly higher OPG expression levels (Fig. 3B–C) in the Adv-OPG-ADSCs compared to the Adv-EGFP group. Additionally, alizarin red staining and ALP staining results showed that Adv-OPG-ADSCs promoted differentiation into osteoblasts (Fig. 3D) and increased ALP activity (Fig. 3E). Furthermore, colony formation and CCK-8 assays showed that OPG gene modification improved the proliferation capacity (Fig. 3F) and cell viability (Fig. 3G) of ADSCs. The construction of OPG-modified ADSCs was therefore deemed successful.

3.4. Adv-OPG-ADSCs promoted bone formation and reduced bone defects in maxilla of osteoporosis rats

The use of OPG-modified ADSCs improved the state of bone tissue. The HE staining results showed that compared with the OVX + PBS group, the OVX + Adv-ADSCs group slightly increased the bone structure density and the number of bone trabeculae, and the OVX + Adv-OPG-ADSCs group significantly increased the bone structure density and the number of bone trabeculae, and new bone formation accelerated the repair of maxilla bone tissue (Fig. 4A). The micro-CT results revealed a significant improvement in the osteoporotic status of the maxilla after the administration of ADSCs and OPG-modified ADSCs, as compared to the OVX + PBS group. In the maxilla of OVX + Adv-OPG-ADSCs group, bone trabeculae increased, bone trabecular compactness increased, new bone formed to fill part of bone defects and reduce bone loss. (Fig. 4B). The BV/TV ratio and BMD values of the OVX + Adv-OPG-ADSCs group showed a significant increase in comparison to the OVX + PBS group. Although the difference was not statistically significant, the values of Tb. Th and Tb.N increased (Fig. 4C).

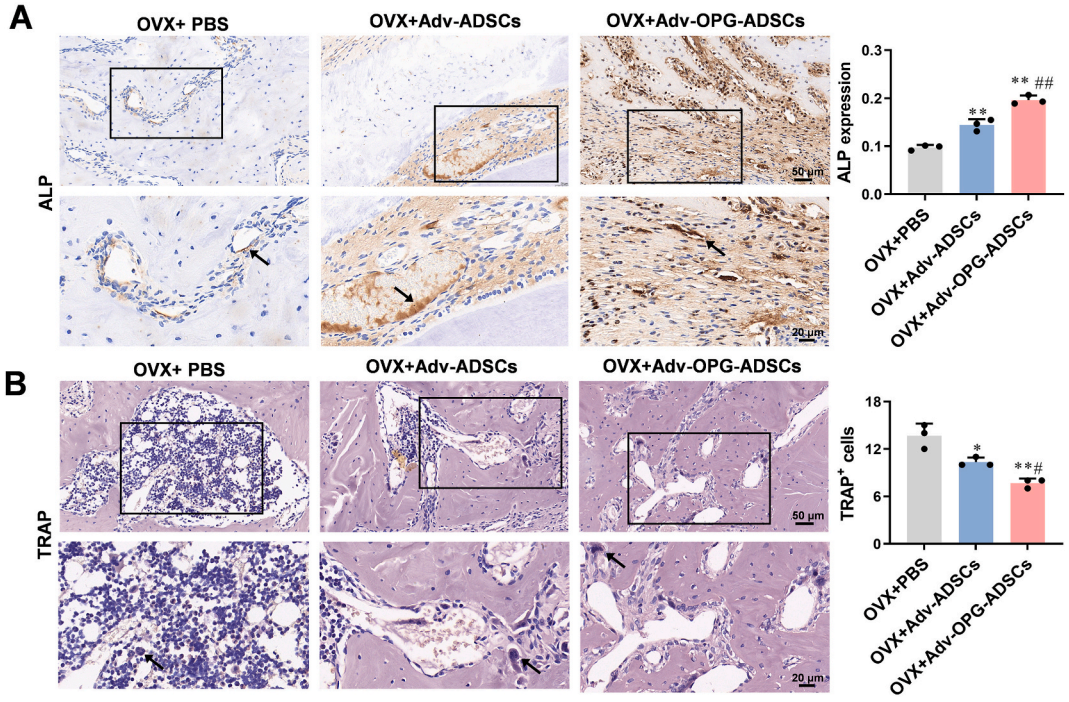

Fig. 5. Adv-OPG-ADSCs repaired osteoporosis caused by oophorectomy by inhibiting osteoclast activity and enhancing osteoblast activity. (A) Analysis of ALP in the maxillary bone of osteoporosis model rats were examined by immunohistochemistry. Scale bars represent 50 μm (upper panel) and 20 μm (lower panel). (B) TRAP staining analysis was performed on the maxillary bone of osteoporosis model rats to identify osteoclasts. Scale bars represent 50 μm (upper panel) and 20 μm (lower panel); All data are mean ± standard deviation, n = 3, **P < 0.01, compared with OVX + PBS group; $^{\#}$P < 0.05, $^{\#\#}$P < 0.01, compared with OVX + Adv-ADSCs group.

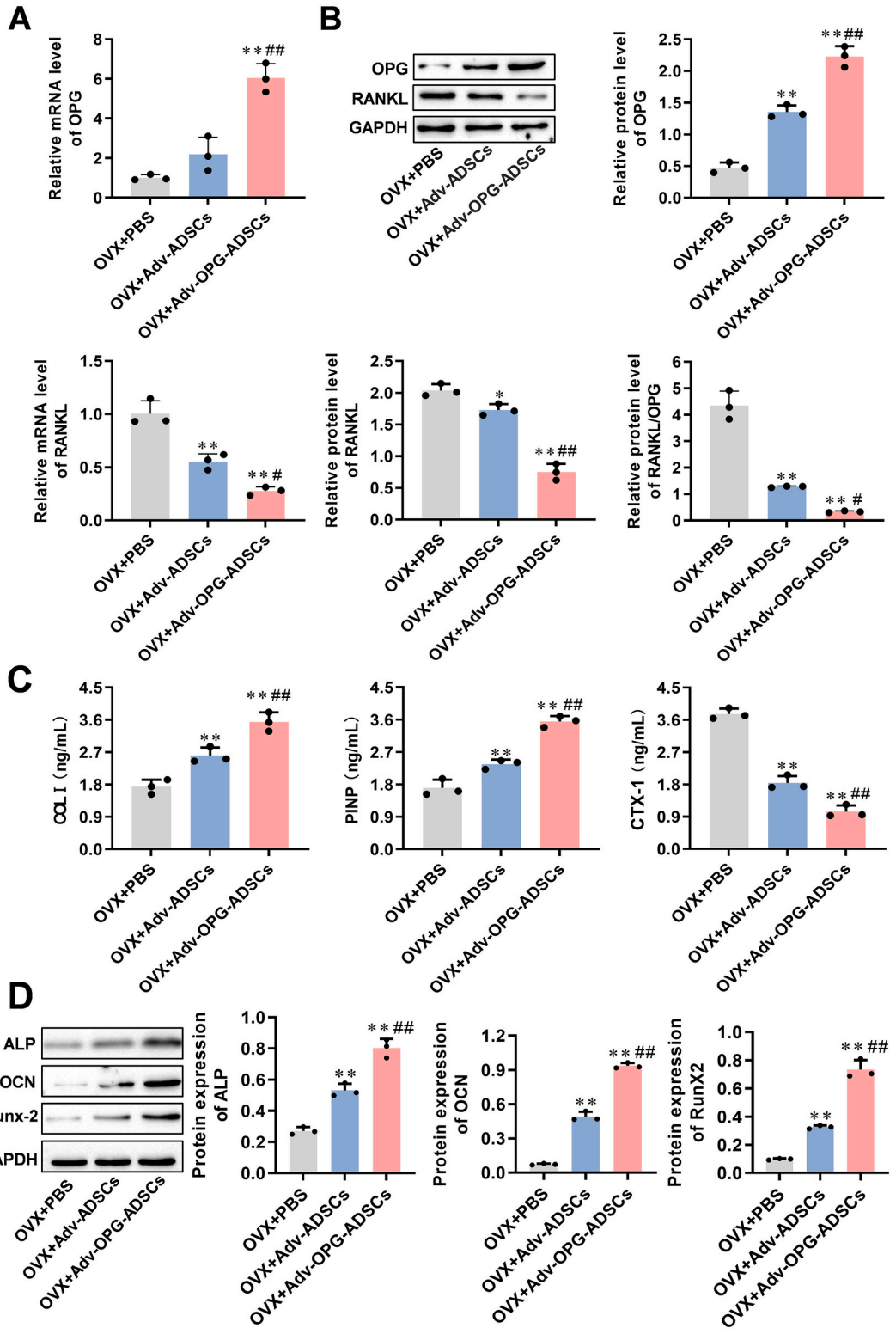

Fig. 6. Adv-OPG-ADSCs promoted bone formation, inhibit bone resorption, and ultimately facilitate bone repair. (A–B) Analysis of the expression levels of OPG and RANKL in bone tissue around maxillary teeth by RT-qPCR and Western blotting. (C) The concentrations of COL I, PINP and CTX-I were detected by ELISA. (D) Analysis of the expression levels of ALP, OCN and Runx-2 in bone tissue around maxillary teeth by Western blotting; All data are mean ± standard deviation, n = 3, $^{**}P < 0.01$, compared with OVX + PBS group; $^{\#}P < 0.05$, $^{\#\#}P < 0.01$, compared with OVX + Adv-ADSCs group.

3.5. Adv-OPG-ADSCs repaired osteoporosis caused by oophorectomy by inhibiting osteoclast activity and enhancing osteoblast activity

The therapeutic effect of bone repair was verified by detecting markers of osteoblasts and osteoclasts. The ALP staining results, based on positive staining in brownish-yellow, showed that OPG-modified ADSCs significantly increased ALP expression compared to the OVX + PBS group and OVX + Adv-ADSCs group (Fig. 5A). Osteoclast results indicated that Adv-OPG-ADSCs significantly reduced TRAP expression compared to the OVX + PBS group and OVX + Adv-ADSCs group (Fig. 5B), indicating that osteoclast differentiation was inhibited.

3.6. Adv-OPG-ADSCs promote bone formation, inhibit bone resorption, and ultimately facilitate bone repair

Furthermore, RT-qPCR and Western blotting were performed on the expression levels of OPG and RANKL. The mRNA level and protein level of OPG in the OVX + Adv-OPG-ADSCs group were significantly elevated compared to those in the OVX + PBS group and the OVX + Adv-ADSCs group (Fig. 6A–B). The mRNA expression level of RANKL was significantly reduced in comparison to the OVX + PBS group and the OVX + Adv-ADSCs group. The protein level of RANKL was also significantly reduced compared to the OVX + PBS group and the OVX + Adv-ADSCs group. The RANKL/OPG ratio also decreased significantly after treating OPG-modified ADSCs compared to the OVX + PBS group and the OVX + Adv-ADSCs group. With the treatment of Adv-OPG-ADSCs, the concentrations of COL I and PINP significantly increased, while the concentration of CTX-1 significantly decreased (Fig. 6C). Osteogenic markers showed that the expression of ALP, OCN, and Runx-2 in the OVX + Adv-OPG-ADSCs group was significantly higher than that in the OVX group and OVX + Adv-ADSCs group, as revealed by Western blot results (Fig. 6D). These results indicate that Adv-OPG-ADSCs enhance bone formation and inhibit bone resorption in the osteoporotic maxillary bone.

4. Discussion

In our study, we have successfully constructed ADSCs with high expression of OPG, which significantly improved the morphology of the maxilla caused by estrogen deficiency in implant teeth. Additionally, we observed a significant increase in the formation of osteoblasts and inhibition of osteoclast generation. These results further improved the bone formation after implant teeth, providing a basis for clinical dental implant treatment of tooth loss in osteoporosis patients.

Osteoporosis, which is particularly common in postmenopausal women, is mainly related to excessive bone resorption caused by postmenopausal bone loss associated with estrogen deficiency [6]. Osteoblasts and osteoclasts both have estrogen receptors [23], which means that estrogen can bind to homologous estrogen receptors in the nucleus and directly regulate the transcription of genes or bind to translation factors [24]. Estrogen binding to membrane receptors can also regulate the apoptosis of osteoclasts, osteoblasts and osteocytes [24]. Our histological and micro-CT results are consistent in that both indicate that estrogen deficiency after double oophorectomy causes osteoporosis in the rat maxilla, with a reduction in trabecular number and decreased density of bone structures in the maxilla.

Both ADSCs and bone marrow derived stem cells (BMSCs) have the potential to differentiate into osteoblasts [25]. However, the easy separation of ADSCs results in higher genetic and morphological stability, higher proliferative activity, more effective collagen production, and higher tolerance to cell apoptosis in long-term culture [26,27]. Many studies have reported that genetically modified ADSCs can be used to treat bone metabolic diseases. In a rat model, ADSCs overexpressing bone morphogenetic proteins can induce bone tissue regeneration and accelerate vertebral repair [9]. In a rabbit model with radial defect, Runx-2 gene modified rabbit ADSCs exhibit excellent bone induction ability in the treatment of bone defects [28]. Similarly, in our study, we also use OPG gene modified ADSCs to promote bone formation and reduce bone defects in the maxillary teeth of osteoporotic rats after implantation. In addition, due to its low immunogenicity and regulatory effects, ADSC is suitable for clinical applications in allogeneic transplantation and immunotherapy for drug-resistant immune diseases [29,30].

The adenovirus are the most efficient vector for gene transfer vector and is commonly used to introduce exogenous genetic information into cells [17,31]. Adenovirus vectors have the ability to infect both dividing and non-dividing cells and promote extended target gene expression with high transfection efficiency and low toxicity [32,33]. For our study, we selected ADSC as the donor cell and transfected it with an adenovirus vector. A gene therapy study using adenovirus vectors revealed that therapeutic gene expression levels gradually decrease after delivery, ultimately resulting in the disappearance of bone induction effects [17]. These characteristics help to prevent the activation of oncogenes and adverse effects caused by indefinite transgenic expression. Therefore, in our study, we also opted to use ADSCs as carriers for OPG genes rather than direct gene delivery. However, some studies have shown that adenoviruses containing target genes can be directly delivered to the regenerative site, which could lead to ectopic bone growth, requiring further evaluation [34].

Bone reconstruction involves the stages of bone formation and resorption, which always maintain a balance between the amount of bone resorption and the amount of bone formation. These two stages are regulated by coupling factors such as RANKL, which link bone resorption and formation to maintain bone homeostasis [35]. An imbalanced regulation of the bone remodeling process can lead to metabolic bone diseases. Osteoporosis is one such metabolic disease of bones, which occurs when there is a loss of balance between bone resorption and bone formation [36]. Osteoclast and osteoblasts regulate bone metabolism, and osteoclast absorb bone, while osteoblasts synthesize and fill bone matrix [36]. The amount of bone depends on the interaction of these cells. Osteoporosis is characterized by relatively normal osteoclast activity and a significant decrease in the number and activity of osteoblasts [37,38]. Decreased estrogen secretion can lead to a decrease in OPG secretion in osteoblasts, accelerating bone absorption [39]. RANKL can bind to its receptor RANK and induce osteoclast differentiation, fusion, and activation [40]. RANKL inhibition can improve muscle

strength, insulin sensitivity, and restore bone mass [41]. OPG can prevent RANKL from binding to RANK, and inhibit osteoclast activity and maturation to reduce excessive bone resorption. Therefore, the ratio of RANKL/OPG determines bone quality and bone integrity [42]. The ratio of RANKL to OPG could be affected by various cytokines in the inflammatory tissue, such as IL-6, TNF-α, prostaglandin E2 and IL-1 [43]. In our study, we established an osteoporosis rat model by ovariectomy, and found that OPG was downregulated, RANKL was upregulated, RANK was upregulated, osteoblasts were significantly reduced, and osteoclasts were increased in its maxilla. In a mouse model of oophorectomy, bone volume was significantly increased and osteoclasts were reduced using recombinant adenovirus vectors carrying OPG cDNA [44]. OPG is a bone promoting factor that can be used as an osteogenic supplement to activate the osteogenic ability of undifferentiated hMSCs, thereby enhancing the osteogenic effect of bone tissue engineering [45].

The Osteoprotegerin gene-modified BMSCs have high expression of OPG and promote the osteogenic differentiation of BMSCs [46]. The exogenous supplementation of OPG partially restored β-cell proliferation in IUGR rats, which may be associated with the regulation of the PI3K/AKT/FoxO1 signaling pathway [47]. In our research, it was also found that overexpression of OPG enhanced the cell viability, cell proliferation, and osteogenic differentiation ability of ADSCs. The specific mechanism through which OPG promotes the proliferation of BMSCs and ADSCs stem cells has not been reported, and further research is required.

Osteoblasts are an important source of OPG [48]. In addition to producing new bone matrix, osteoblasts also play a positive role by inhibiting RANKL activity during the resorption phase to terminate bone remodeling cycle [48]. Additionally, research has shown that ADSCs secrete abundant osteoprotegerin [49], and ADSCs-exo reduces the expression levels of RANKL and the ratio of genes RANKL/OPG, and can also antagonize bone cell apoptosis induced by H/SD and bone cell-mediated osteoclastogenesis [50]. In our research, it was observed that, when compared to the OVX + PBS group, Adv-ADSCs were able to reduce the number of Maxilla Osteoclasts and increase the number of osteoblasts in osteoporotic rats. According to related studies, OPG regulates at least two different pathways, one inducing cell proliferation through ERK signaling, and the other inducing angiogenesis through Src signaling [51]. The integrity of the skeleton relies on tight spatial and temporal connections between blood vessels and bone cells [52]. There exists a complex relationship between bone formation and angiogenesis, and the interaction between osteogenesis and angiogenesis has been proven to play a crucial role in bone regeneration [53,54]. In our study, by constructing ADSCs modified with high expression OPG to treat osteoporosis, Adv-OPG-ADSCs increased the expression of OPG, reduced the expression of RANKL, inhibited the activation of osteoclasts, promoted the generation of osteoblasts and promoted the formation of new bones (Fig. 7).

Type I collagen (COL I) is the main organic matrix of bone and can provide rigidity for bone. The N-terminal propeptide (PINP) of COL I and the C-terminal peptide (CTX-1) of the degradation product COL I are markers of bone formation and absorption [55]. During osteogenesis, other osteogenic markers, such as alkaline phosphatase (ALP), osteopontin (OPN), and runt-related transcription factor 2 (Runx-2), also contribute to osteoblast differentiation and bone formation [56,57]. Runx2 is the main molecule that regulates osteoblast differentiation [58]. ALP and Osteonectin are markers of early bone progenitor cells, while OPN and OCN are markers of immature and mature osteoblasts, respectively [59]. In our study, we verified that Adv-OPG-ADSCs increased the expressions of ALP, OCN and Runx-2, increased the concentrations of PINP and COL I, and decreased the concentration of CTX-1 after dental implantation. This indicates that Adv-OPG-ADSCs inhibited bone resorption of osteoclasts and promoted bone formation of osteoblasts, further clarifying the role of Adv-OPG-ADSCs in bone repair after dental implantation.

Through the means of cell therapy and gene technology, this study applied an OPG gene modified ADSCs to promote bone regeneration in the tooth implantation process of osteoporotic rats. This method provides a valuable repair strategy for clinical

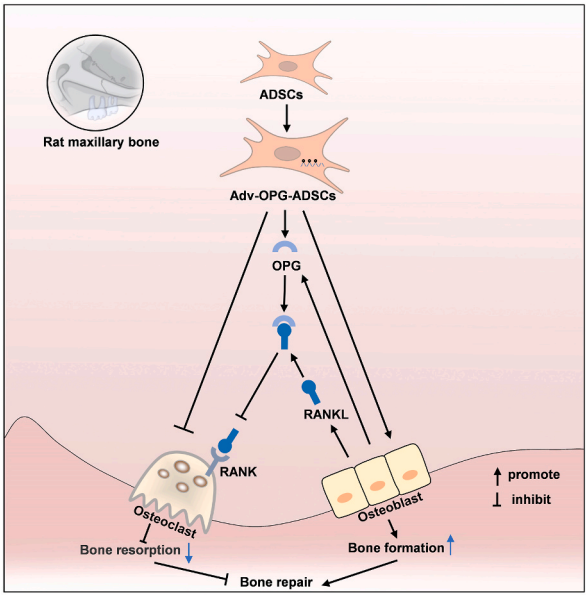

Fig. 7. Rationale of Adv-OPG-ADSCs in the treatment of osteoporosis in rats.

application of dental implants, especially for patients with osteoporosis. However, the widespread clinical application of ADSCs depends on their mode of use. Purification or placement in their microenvironment is crucial for their therapeutic results and may ensure understanding of the side effects caused. Another issue is the transition of ADSC use from autologous environment to allogeneic environment [60]. The development of biotechnology has improved the use of high-purity ADSCs and newly processed cells, which have been proposed for use in allogeneic environments lacking available autologous cells [61]. In this way, ADSCs may play an important role in future medicine, but on the condition that risk factors related to their operation and cryopreservation, concentration, and administration routes are controlled and standardized [60]. ADSCs have been used in various cartilage and bone regenerations, and we will further investigate the role of ADSCs in osteoporosis, providing a scientific basis for subsequent applications.

5. Conclusion

Our results indicated that the intervention of Adv-OPG-ADSCs in rats undergoing OVX, promoted the formation of osteoblasts and inhibited the activation of osteoclasts, thus inhibiting bone absorption and promoting bone formation. The study suggests that Adv-OPG-ADSCs could significantly improve the bone repair of the maxilla after osteoporosis caused by estrogen deficiency following dental implantation, and provide a scientific reference for the follow-up dental implantation of elderly people with osteoporosis.

Funding

This study was supported by the Natural Science Foundation of Ningxia (No.: 2020AAC03358).

Data availability

Data will be made available on request.

Author contributions statement

Xiaoqian Guo conceived and designed the experiments; Yingbiao Wan and Chen Hu performed the experiments; Yingbiao Wan, Chen Hu, Yongjie Hou, Chenchen Si, and Qian Zhao analyzed and interpreted the data; Zhenzhen Wang and Liyuan Wang contributed reagents, materials, analysis tools or data; Yingbiao Wan and Chen Hu wrote the paper; Xiaoqian Guo revised it critically for important intellectual content; All authors read and approved the final manuscript.

Declaration of competing interest

The authors declare that they have no known competing financial interests or personal relationships that could have appeared to influence the work reported in this paper.

Appendix A. Supplementary data

Supplementary data to this article can be found online at https://doi.org/10.1016/j.heliyon.2023.e19474.

References

[1] J.A. Kanis, C. Cooper, R. Rizzoli, J.Y. Reginster, European guidance for the diagnosis and management of osteoporosis in postmenopausal women, Osteoporos. Int. 30 (1) (2019) 3–44.
[2] F. Cosman, The prevention and treatment of osteoporosis: a review, MedGenMed 7 (2) (2005) 73.
[3] L. Warming, C. Hassager, C. Christiansen, Changes in bone mineral density with age in men and women: a longitudinal study, Osteoporos. Int. 13 (2) (2002) 105–112.
[4] J. Guo, Y. Huang, S. Bian, C. Zhao, Y. Jin, D. Yu, et al., Associations of urinary polycyclic aromatic hydrocarbons with bone mass density and osteoporosis in U.S. adults, NHANES 2005-2010, Environ. Pollut. 240 (2018) 209–218.
[5] M.N. Weitzmann, R. Pacifici, Estrogen deficiency and bone loss: an inflammatory tale, J. Clin. Invest. 116 (5) (2006) 1186–1194.
[6] Michael R. McClung, V. JoAnn, Pinkerton, Jennifer Blake, Cosman Felicia A, Lewiecki E Michael, Marla Shapiro, Management of osteoporosis in postmenopausal women: the 2021 position statement of the North American Menopause Society, Menopause 28 (9) (2021) 973–997.
[7] K. Huang, H.L. Cai, J.P. Bao, L.D. Wu, Dehydroepiandrosterone and age-related musculoskeletal diseases: connections and therapeutic implications, Ageing Res. Rev. 62 (2020), 101132.
[8] L. Jiang, W. Zhang, L. Wei, Q. Zhou, G. Yang, N. Qian, et al., Early effects of parathyroid hormone on vascularized bone regeneration and implant osseointegration in aged rats, Biomaterials 179 (2018) 15–28.
[9] D. Sheyn, I. Kallai, W. Tawackoli, D. Cohn Yakubovich, A. Oh, S. Su, et al., Gene-modified adult stem cells regenerate vertebral bone defect in a rat model, Mol. Pharm. 8 (5) (2011) 1592–1601.
[10] A. Skubis, J. Gola, B. Sikora, J. Hybiak, M. Paul-Samojedny, U. Mazurek, et al., Impact of antibiotics on the proliferation and differentiation of human adipose-derived mesenchymal stem cells, Int. J. Mol. Sci. 18 (12) (2017).
[11] M. Nawaz, F. Fatima, K.C. Vallabhaneni, P. Penfornis, H. Valadi, K. Ekström, et al., Extracellular vesicles: evolving factors in stem cell biology, Stem Cell. Int. 2016 (2016), 1073140.

[12] X. Yuan, L. Li, H. Liu, J. Luo, Y. Zhao, C. Pan, et al., Strategies for improving adipose-derived stem cells for tissue regeneration, Burns Trauma 10 (2022), tkac028.
[13] F. Guilak, K.E. Lott, H.A. Awad, Q. Cao, K.C. Hicok, B. Fermor, et al., Clonal analysis of the differentiation potential of human adipose-derived adult stem cells, J. Cell. Physiol. 206 (1) (2006) 229–237.
[14] A.J. Salgado, R.L. Reis, N.J. Sousa, J.M. Gimble, Adipose tissue derived stem cells secretome: soluble factors and their roles in regenerative medicine, Curr. Stem Cell Res. Ther. 5 (2) (2010) 103–110.
[15] X. Wei, Z. Du, L. Zhao, D. Feng, G. Wei, Y. He, et al., IFATS collection: the conditioned media of adipose stromal cells protect against hypoxia-ischemia-induced brain damage in neonatal rats, Stem Cell. 27 (2) (2009) 478–488.
[16] A. Abudusaimi, Y. Aihemaitijiang, Y.H. Wang, L. Cui, S. Maimaitiming, M. Abulikemu, Adipose-derived stem cells enhance bone regeneration in vascular necrosis of the femoral head in the rabbit, J. Int. Med. Res. 39 (5) (2011) 1852–1860.
[17] J.J. Sun, X.H. Zheng, L.Y. Wang, L. Liu, W. Jing, Y.F. Lin, et al., New bone formation enhanced by ADSCs overexpressing hRunx2 during mandibular distraction osteogenesis in osteoporotic rabbits, J. Orthop. Res. 32 (5) (2014) 709–720.
[18] N.G. Kondegowda, R. Fenutria, I.R. Pollack, M. Orthofer, A. Garcia-Ocaña, J.M. Penninger, et al., Osteoprotegerin and denosumab stimulate human beta cell proliferation through inhibition of the receptor activator of NF-κB ligand pathway, Cell Metabol. 22 (1) (2015) 77–85.
[19] J. Xiong, M. Piemontese, M. Onal, J. Campbell, J.J. Goellner, V. Dusevich, et al., Osteocytes, not osteoblasts or lining cells, are the main source of the RANKL required for osteoclast formation in remodeling bone, PLoS One 10 (9) (2015), e0138189.
[20] M. Infante, A. Fabi, F. Cognetti, S. Gorini, M. Caprio, A. Fabbri, RANKL/RANK/OPG system beyond bone remodeling: involvement in breast cancer and clinical perspectives, J. Exp. Clin. Cancer Res. 38 (1) (2019) 12.
[21] A.K. Bengtsson, E.J. Ryan, Immune function of the decoy receptor osteoprotegerin, Crit. Rev. Immunol. 22 (3) (2002) 201–215.
[22] C.E. Lampropoulos, I. Papaioannou, D.P. D'Cruz, Osteoporosis–a risk factor for cardiovascular disease? Nat. Rev. Rheumatol. 8 (10) (2012) 587–598.
[23] E.F. Eriksen, D.S. Colvard, N.J. Berg, M.L. Graham, K.G. Mann, T.C. Spelsberg, et al., Evidence of estrogen receptors in normal human osteoblast-like cells, Science 241 (4861) (1988) 84–86.
[24] L. Li, Z. Wang, Ovarian aging and osteoporosis, Adv. Exp. Med. Biol. 1086 (2018) 199–215.
[25] S.J. Su, K.L. Chang, S.H. Su, Y.T. Yeh, H.W. Shyu, K.M. Chen, Caffeine regulates osteogenic differentiation and mineralization of primary adipose-derived stem cells and a bone marrow stromal cell line, Int. J. Food Sci. Nutr. 64 (4) (2013) 429–436.
[26] L. Frese, P.E. Dijkman, S.P. Hoerstrup, Adipose tissue-derived stem cells in regenerative medicine, Transfus. Med. Hemotherapy 43 (4) (2016) 268–274.
[27] C. Li, S. Wei, Q. Xu, Y. Sun, X. Ning, Z. Wang, Application of ADSCs and their exosomes in scar prevention, Stem Cell Rev Rep 18 (3) (2022) 952–967.
[28] D. Han, J. Li, Repair of bone defect by using vascular bundle implantation combined with Runx II gene-transfected adipose-derived stem cells and a biodegradable matrix, Cell Tissue Res. 352 (3) (2013) 561–571.
[29] K.R. McIntosh, Evaluation of cellular and humoral immune responses to allogeneic adipose-derived stem/stromal cells, Methods Mol. Biol. 702 (2011) 133–150.
[30] B. Puissant, C. Barreau, P. Bourin, C. Clavel, J. Corre, C. Bousquet, et al., Immunomodulatory effect of human adipose tissue-derived adult stem cells: comparison with bone marrow mesenchymal stem cells, Br. J. Haematol. 129 (1) (2005) 118–129.
[31] L. Meinel, S. Hofmann, O. Betz, R. Fajardo, H.P. Merkle, R. Langer, et al., Osteogenesis by human mesenchymal stem cells cultured on silk biomaterials: comparison of adenovirus mediated gene transfer and protein delivery of BMP-2, Biomaterials 27 (28) (2006) 4993–5002.
[32] S. Watanabe, T. Ogasawara, Y. Tamura, T. Saito, T. Ikeda, N. Suzuki, et al., Targeting gene expression to specific cells of kidney tubules in vivo, using adenoviral promoter fragments, PLoS One 12 (3) (2017), e0168638.
[33] J.M. McMahon, S. Conroy, M. Lyons, U. Greiser, C. O'Shea, P. Strappe, et al., Gene transfer into rat mesenchymal stem cells: a comparative study of viral and nonviral vectors, Stem Cell. Dev. 15 (1) (2006) 87–96.
[34] M. Egermann, A.W. Baltzer, S. Adamaszek, C. Evans, P. Robbins, E. Schneider, et al., Direct adenoviral transfer of bone morphogenetic protein-2 cDNA enhances fracture healing in osteoporotic sheep, Hum. Gene Ther. 17 (5) (2006) 507–517.
[35] Y.Q. Liu, Z.L. Hong, L.B. Zhan, H.Y. Chu, X.Z. Zhang, G.H. Li, Wedelolactone enhances osteoblastogenesis by regulating Wnt/β-catenin signaling pathway but suppresses osteoclastogenesis by NF-κB/c-fos/NFATc1 pathway, Sci. Rep. 6 (2016), 32260.
[36] S.Y. Yang, S.H. Lee, B.H. Tai, H.D. Jang, Y.H. Kim, Antioxidant and anti-osteoporosis activities of chemical constituents of the stems of zanthoxylum piperitum, Molecules 23 (2) (2018).
[37] P. Cho, G.B. Schneider, K. Krizan, J.C. Keller, Examination of the bone-implant interface in experimentally induced osteoporotic bone, Implant Dent. 13 (1) (2004) 79–87.
[38] A. Qadir, S. Liang, Z. Wu, Z. Chen, L. Hu, A. Qian, Senile osteoporosis: the involvement of differentiation and senescence of bone marrow stromal cells, Int. J. Mol. Sci. 21 (1) (2020).
[39] S. Bord, D.C. Ireland, S.R. Beavan, J.E. Compston, The effects of estrogen on osteoprotegerin, RANKL, and estrogen receptor expression in human osteoblasts, Bone 32 (2) (2003) 136–141.
[40] X. Zhu, J.J. Gao, E. Landao-Bassonga, N.J. Pavlos, A. Qin, J.H. Steer, et al., Thonzonium bromide inhibits RANKL-induced osteoclast formation and bone resorption in vitro and prevents LPS-induced bone loss in vivo, Biochem. Pharmacol. 104 (2016) 118–130.
[41] N. Bonnet, L. Bourgoin, E. Biver, E. Douni, S. Ferrari, RANKL inhibition improves muscle strength and insulin sensitivity and restores bone mass, J. Clin. Invest. 129 (8) (2019) 3214–3223.
[42] B.F. Boyce, L. Xing, Biology of RANK, RANKL, and osteoprotegerin, Arthritis Res. Ther. 9 (Suppl 1) (2007) S1. Suppl 1.
[43] S.A. Hienz, S. Paliwal, S. Ivanovski, Mechanisms of bone resorption in periodontitis, J Immunol Res 2015 (2015), 615486.
[44] B. Bolon, C. Carter, M. Daris, S. Morony, C. Capparelli, A. Hsieh, et al., Adenoviral delivery of osteoprotegerin ameliorates bone resorption in a mouse ovariectomy model of osteoporosis, Mol. Ther. 3 (2) (2001) 197–205.
[45] S. Palumbo, W.J. Li, Osteoprotegerin enhances osteogenesis of human mesenchymal stem cells, Tissue Eng. 19 (19–20) (2013) 2176–2187.
[46] X. Liu, C. Bao, H.H.K. Xu, J. Pan, J. Hu, P. Wang, et al., Osteoprotegerin gene-modified BMSCs with hydroxyapatite scaffold for treating critical-sized mandibular defects in ovariectomized osteoporotic rats, Acta Biomater. 42 (2016) 378–388.
[47] S. Tang, Y. Xin, M. Yang, D. Zhang, C. Xu, Osteoprotegerin promotes islet β cell proliferation in intrauterine growth retardation rats through the PI3K/AKT/FoxO1 pathway, Int. J. Clin. Exp. Pathol. 12 (6) (2019) 2324–2338.
[48] K.M. Cawley, N.C. Bustamante-Gomez, A.G. Guha, R.S. MacLeod, J. Xiong, I. Gubrij, et al., Local production of osteoprotegerin by osteoblasts suppresses bone resorption, Cell Rep. 32 (10) (2020), 108052.
[49] M.B. Dov, B. Krief, M. Benhamou, A. Klein, S. Schwartz, A. Loewenstein, et al., Regenerative effect of adipose derived mesenchymal stem cells on ganglion cells in the hypoxic organotypic retina culture, Int J Stem Cells 16 (2) (2023) 244–249.
[50] L. Ren, Z.J. Song, Q.W. Cai, R.X. Chen, Y. Zou, Q. Fu, et al., Adipose mesenchymal stem cell-derived exosomes ameliorate hypoxia/serum deprivation-induced osteocyte apoptosis and osteocyte-mediated osteoclastogenesis in vitro, Biochem. Biophys. Res. Commun. 508 (1) (2019) 138–144.
[51] M. Kobayashi-Sakamoto, E. Isogai, I. Holen, Osteoprotegerin induces cytoskeletal reorganization and activates FAK, Src, and ERK signaling in endothelial cells, Eur. J. Haematol. 85 (1) (2010) 26–35.
[52] L. Rochette, A. Meloux, E. Rigal, M. Zeller, Y. Cottin, C. Vergely, The role of osteoprotegerin and its ligands in vascular function, Int. J. Mol. Sci. 20 (3) (2019).
[53] V. Veeriah, R. Paone, S. Chatterjee, A. Teti, M. Capulli, Osteoblasts regulate angiogenesis in response to mechanical unloading, Calcif. Tissue Int. 104 (3) (2019) 344–354.
[54] A.P. Kusumbe, S.K. Ramasamy, R.H. Adams, Coupling of angiogenesis and osteogenesis by a specific vessel subtype in bone, Nature 507 (7492) (2014) 323–328.
[55] R. Eastell, P. Szulc, Use of bone turnover markers in postmenopausal osteoporosis, Lancet Diabetes Endocrinol. 5 (11) (2017) 908–923.
[56] T. Komori, Signaling networks in RUNX2-dependent bone development, J. Cell. Biochem. 112 (3) (2011) 750–755.
[57] G.S. Stein, J.B. Lian, T.A. Owen, Relationship of cell growth to the regulation of tissue-specific gene expression during osteoblast differentiation, Faseb. J. 4 (13) (1990) 3111–3123.

[58] T. Fujita, Y. Azuma, R. Fukuyama, Y. Hattori, C. Yoshida, M. Koida, et al., Runx2 induces osteoblast and chondrocyte differentiation and enhances their migration by coupling with PI3K-Akt signaling, J. Cell Biol. 166 (1) (2004) 85–95.
[59] T. Komori, H. Yagi, S. Nomura, A. Yamaguchi, K. Sasaki, K. Deguchi, et al., Targeted disruption of Cbfa1 results in a complete lack of bone formation owing to maturational arrest of osteoblasts, Cell 89 (5) (1997) 755–764.
[60] L. Mazini, L. Rochette, M. Amine, G. Malka, Regenerative capacity of adipose derived stem cells (ADSCs), comparison with mesenchymal stem cells (MSCs), Int. J. Mol. Sci. 20 (10) (2019).
[61] H.J. Duckers, K. Pinkernell, A.M. Milstein, M.H. Hedrick, The Bedside Celution system for isolation of adipose derived regenerative cells, EuroIntervention 2 (3) (2006) 395–398.